

Supplemental information

Parsing the role of NSP1 in SARS-CoV-2 infection

Tal Fisher, Avi Gluck, Krishna Narayanan, Makoto Kuroda, Aharon Nachshon, Jason C. Hsu, Peter J. Halfmann, Yfat Yahalom-Ronen, Hadas Tamir, Yaara Finkel, Michal Schwartz, Shay Weiss, Chien-Te K. Tseng, Tomer Israely, Nir Paran, Yoshihiro Kawaoka, Shinji Makino, and Noam Stern-Ginossar

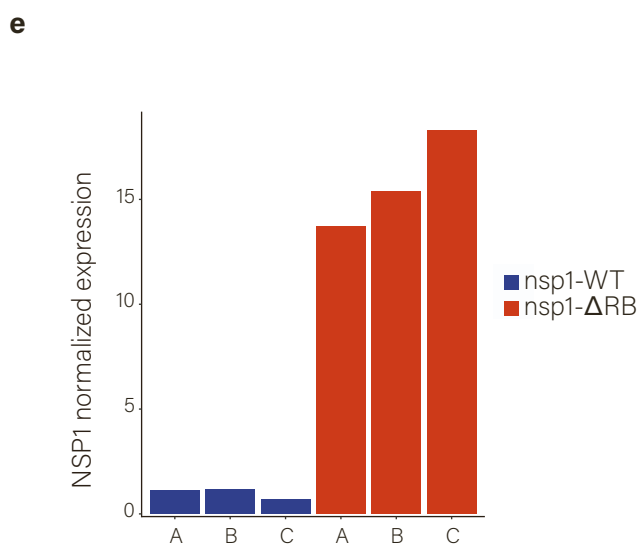
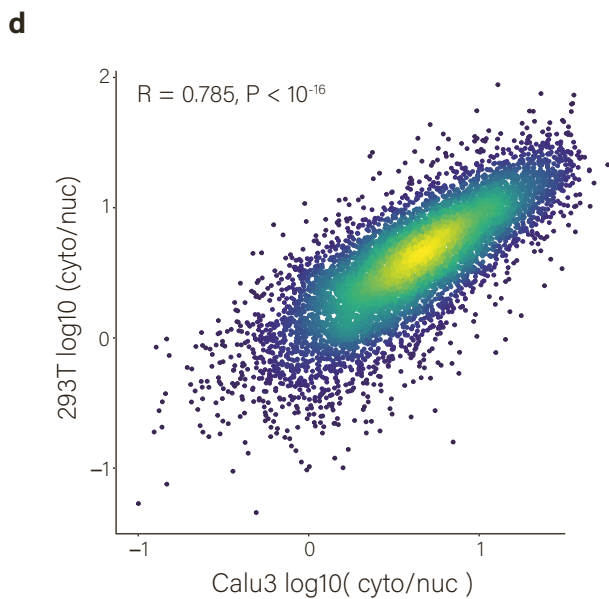
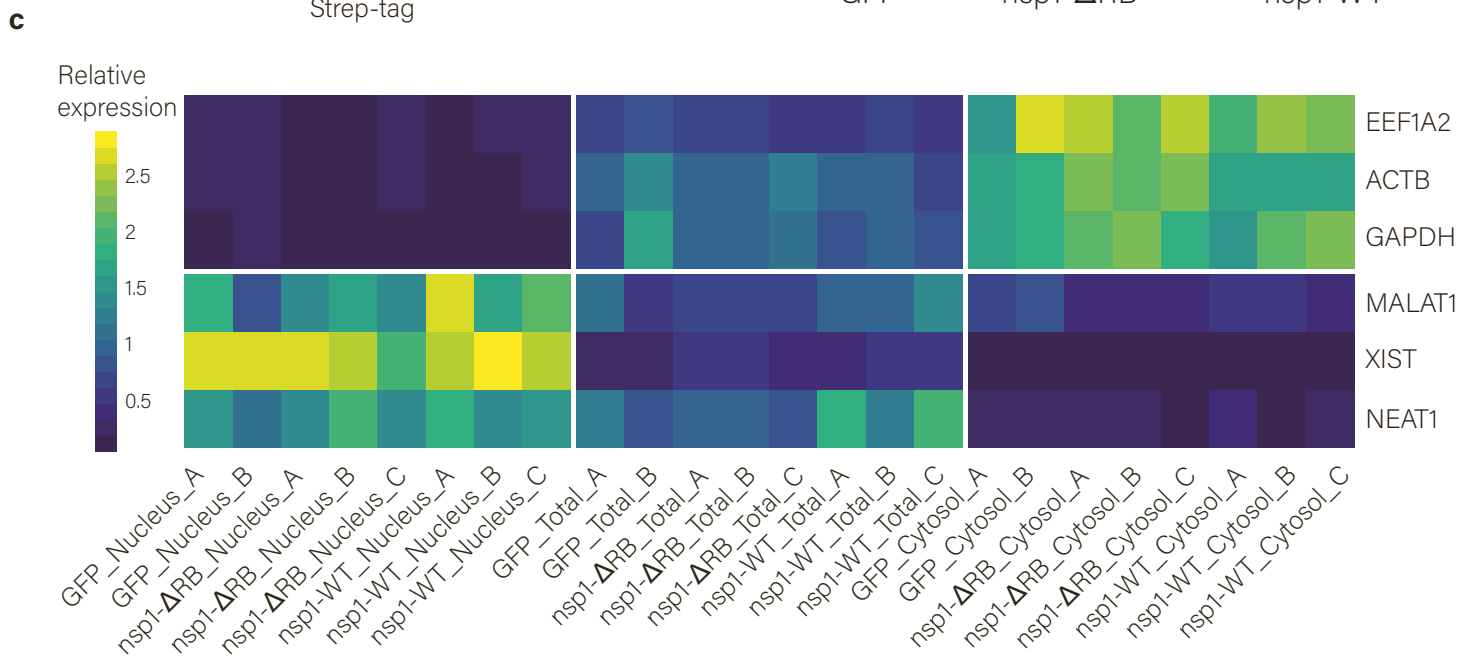
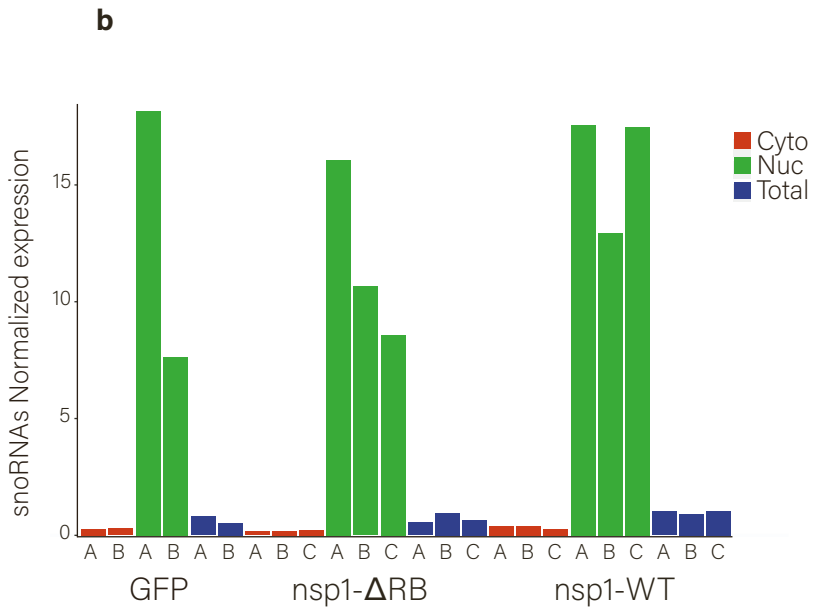
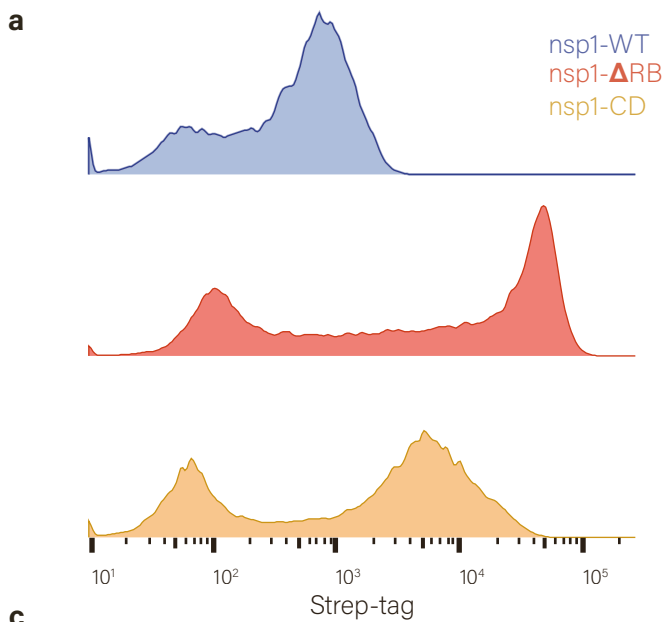


Figure S1. Nsp1 inhibits its own expression, related to Figures 1 and 2.

a. Flow cytometry analysis of the Strep tag expression in cells transfected with nsp1-WT, nsp1- Δ RB, or nsp1-CD containing strep-tag at the C-terminus. **b.** Normalized sum of the expression of snoRNAs in the nuclear (Nuc), cytosolic (Cyto), and total fractions of 293T cells transfected with nsp1-WT, nsp1- Δ RB, or GFP with A, B and C representing biological replicates. **c.** Heatmap showing the relative expression of cellular mRNAs (EEF1A2, ACTB, GAPDH) and nuclear lncRNAs (MALAT1, XIST, NEAT1) in the nuclear (left panels), cytosolic (right panels), and total (middle panels) fractions of 293T cells transfected with nsp1-WT, nsp1- Δ RB, or GFP. **d.** Scatter plot of transcript cyto/nuc ratios calculated from fractionation measurements in 293T cells transfected with plasmid expressing GFP relative to cyto/nuc ratios measured in Calu3 cells (Finkel et al., 2021a). R (pearson) and two-sided P value are presented. **e.** Expression of transcripts encoding nsp1 calculated from RNA-seq data. Expression of nsp1-WT transcripts or nsp1- Δ RB transcripts was normalized to NEAT1 RNA (a nuclear long non coding RNA), and nsp1- Δ RB expression relative to the mean of nsp1-WT samples are presented.

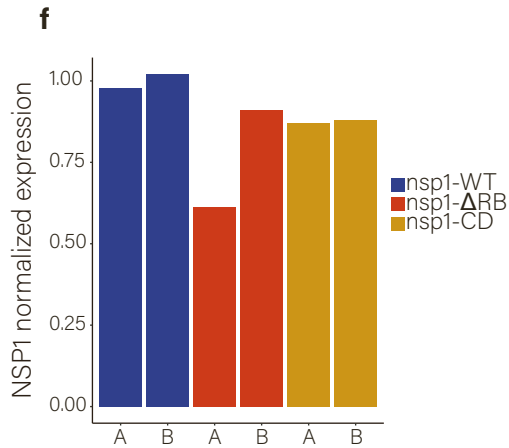
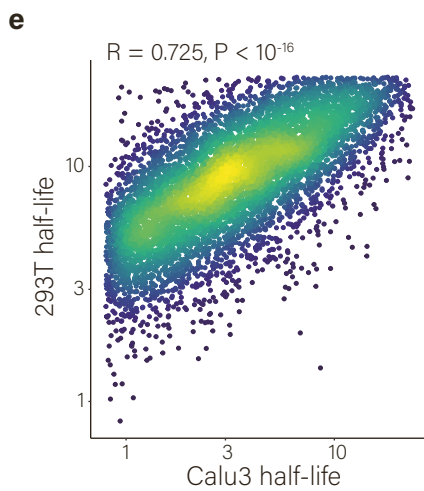
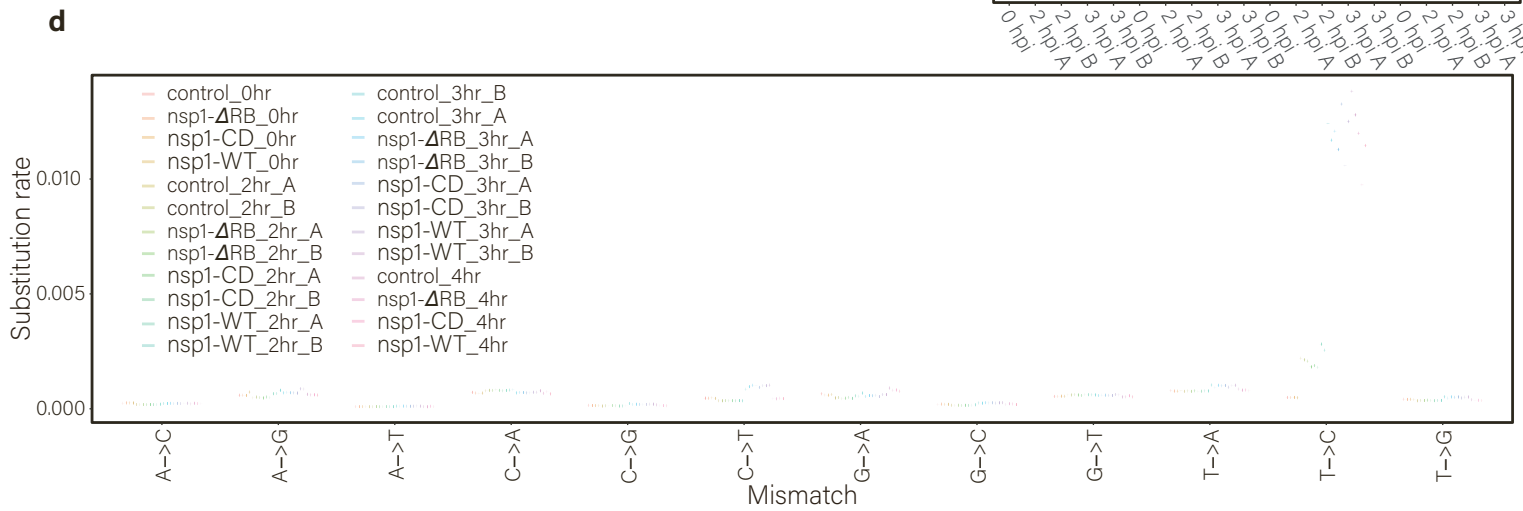
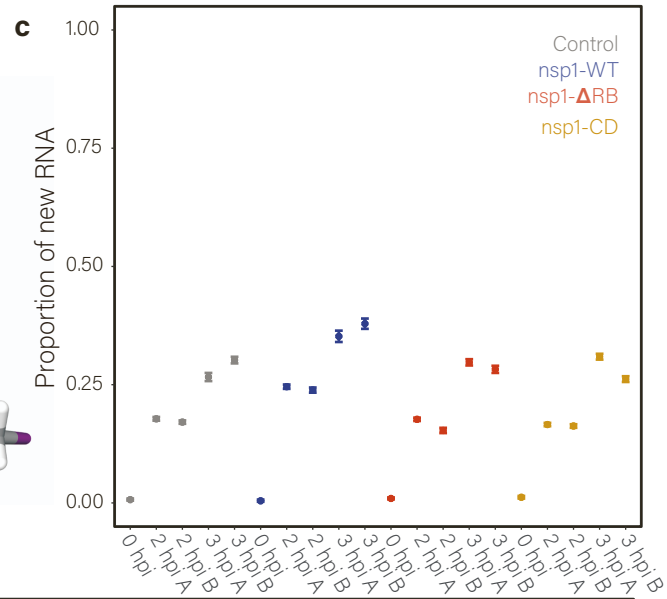
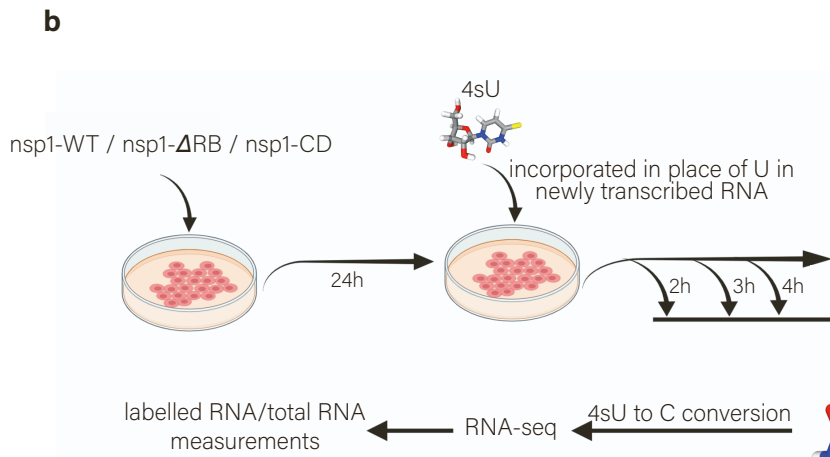
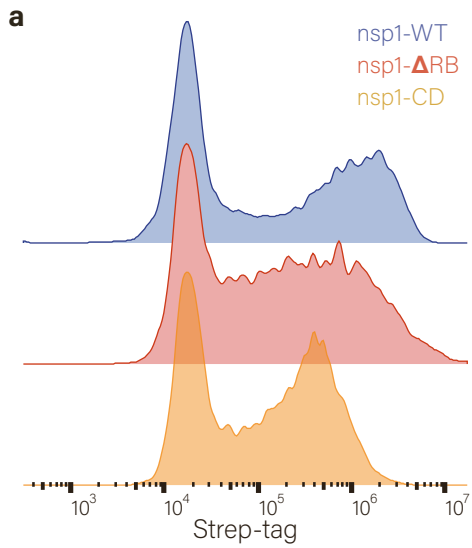
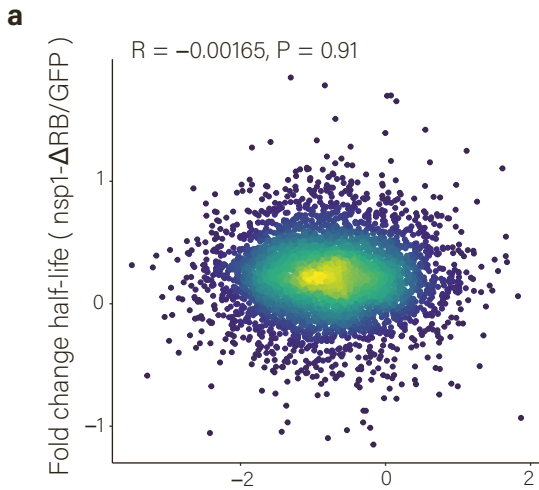
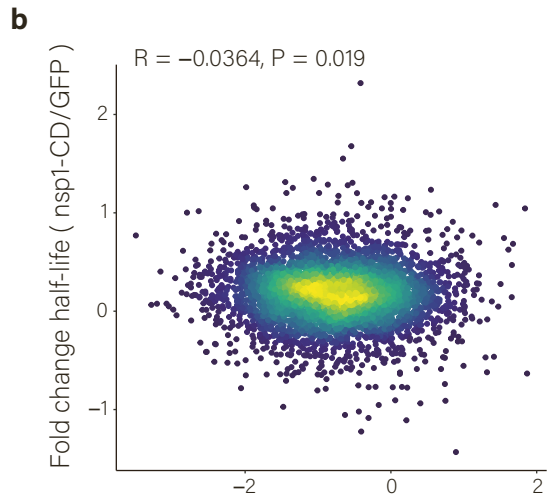


Figure S2. Subcellular fractionation and SLAM-seq measurements in nsp1 expressing cells, related to Figure 2.

a. Flow cytometry analysis of the Strep tag-positive cells, in cells transfected with plasmid expressing nsp1-WT, nsp1- Δ RB, or nsp1-CD, all of which were cloned downstream to the CoV2 viral 5' leader sequence. **b.** Experimental design of the SLAM-seq measurements and the half-life calculation. **c.** Rates of nucleotide substitutions demonstrate efficient conversion rates in 4sU-treated samples compared to non-treated cells (no 4sU). **d.** Proportion of new-to-total RNA (NTR) in 293T cells transfected with plasmid expressing GFP, nsp1-WT, nsp1- Δ RB, or nsp1-CD as calculated by GRAND-SLAM(Jürges et al., 2018). **e.** Scatter plot of transcript half-lives calculated from SLAM-seq measurements in 293T cells transfected with plasmid expressing GFP relative to transcript half-lives in Calu3 cells(Finkel et al., 2021a). Pearson's R and two-sided P-value are presented. **f.** Expression levels of nsp1 transcripts calculated from RNA-seq data. Nsp1 expression in each of the conditions (nsp1-WT, nsp1- Δ RB, or nsp1-CD) was normalized to NEAT1 expression, and nsp1 expression relative to the mean of nsp1-WT samples are presented.



Finkel et al. fold change half-life (infected/uninfected)



Finkel et al. fold change half-life (infected/uninfected)

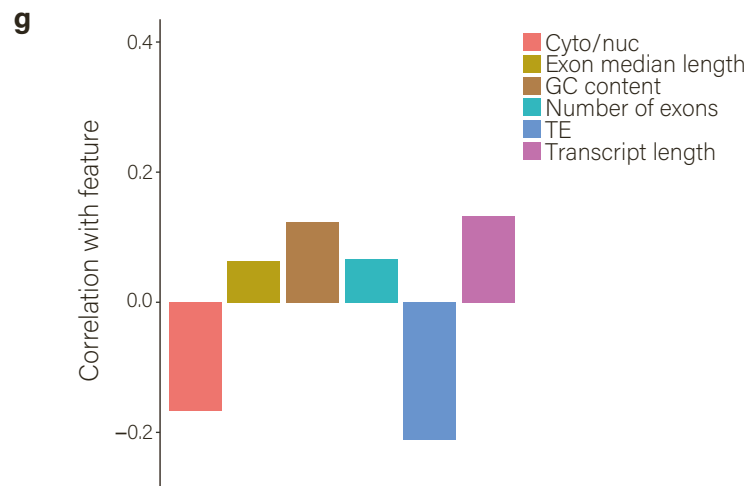
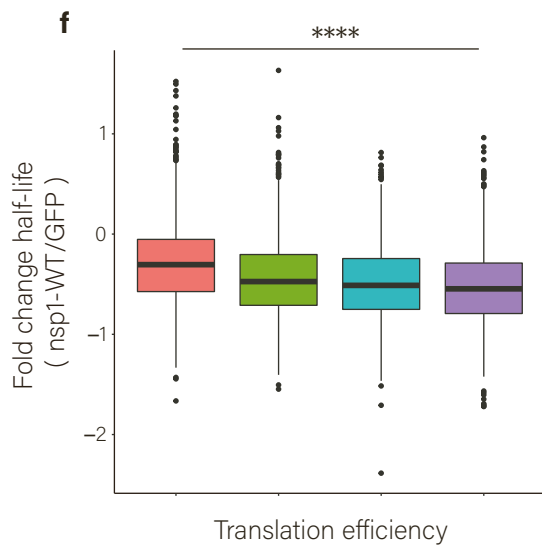
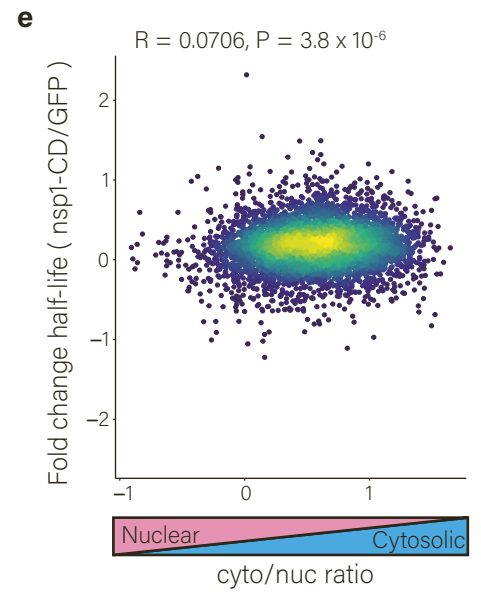
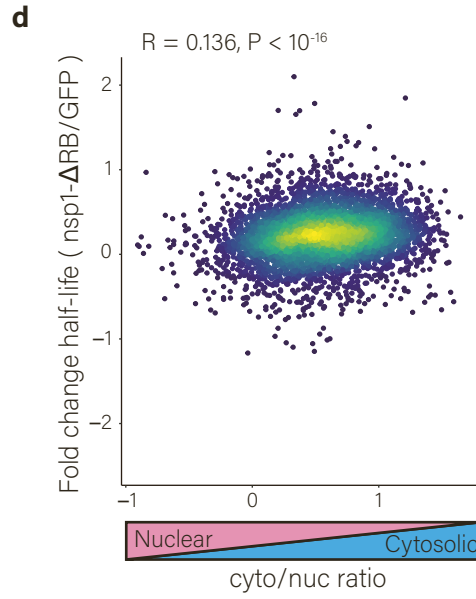
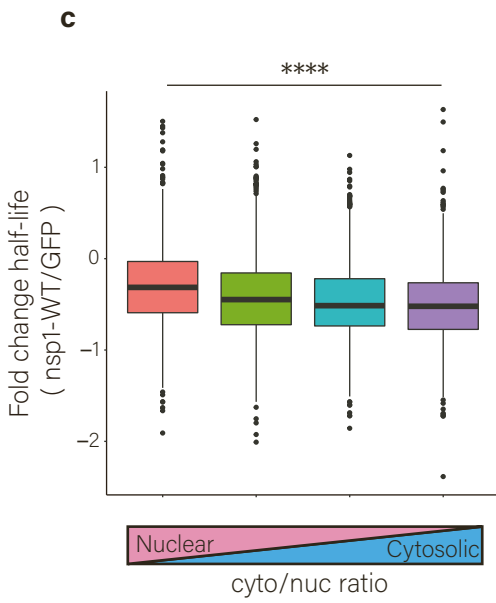


Figure S3. Analysis of gene expression in cells expressing nsp1- Δ RB or nsp1-CD, related to Figure 2.

a and b. Scatter plot of fold change in transcript half-lives in 293T cells transfected with plasmid expressing nsp1- Δ RB (**a**) or nsp1-CD (**b**) relative to those transfected with plasmid expressing GFP and the fold change transcript half-lives in uninfected and infected cells (Finkel et al., 2021a). Pearson's R and two-sided P values are presented. **c.** The nsp1-WT/GFP half-life fold-change compared to the cytosolic/nuclear ratio, divided into 4 bins. P values for two tailed t-tests between extreme bins are presented, **** = $p < 0.0001$. **d and e.** Scatter plot of fold change in transcript half-lives in 293T cells transfected with a plasmid expressing nsp1- Δ RB (**d**) or nsp1-CD (**e**) relative to those transfected with a plasmid expressing GFP and cyto/nuc ratios of uninfected cells (Finkel et al., 2021a). Pearson's R and two-sided P values are presented. **f.** The nsp1-WT/GFP half-life fold-change compared to translation efficiency, divided into 4 bins. P values for two tailed t-tests between extreme bins are presented. **g.** Correlation between gene features and the fold change of transcript half-lives between 293T transfected with a plasmid expressing nsp1-WT or control plasmid.

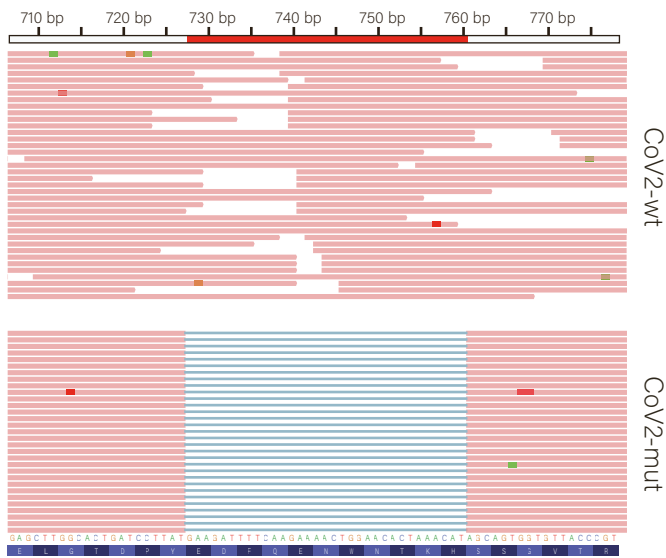
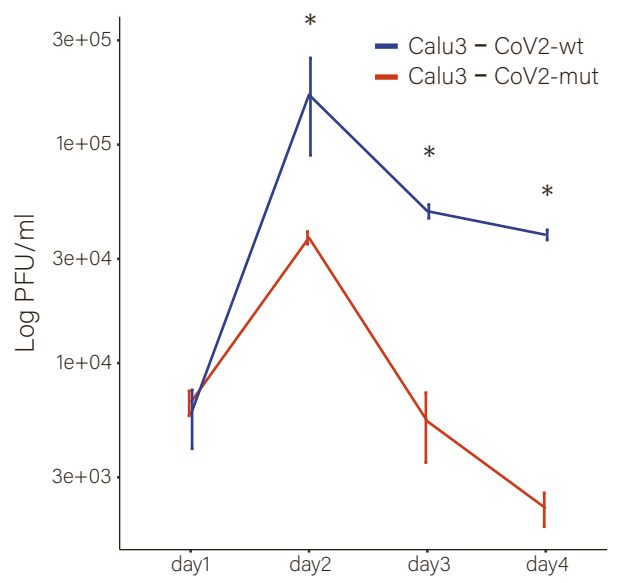
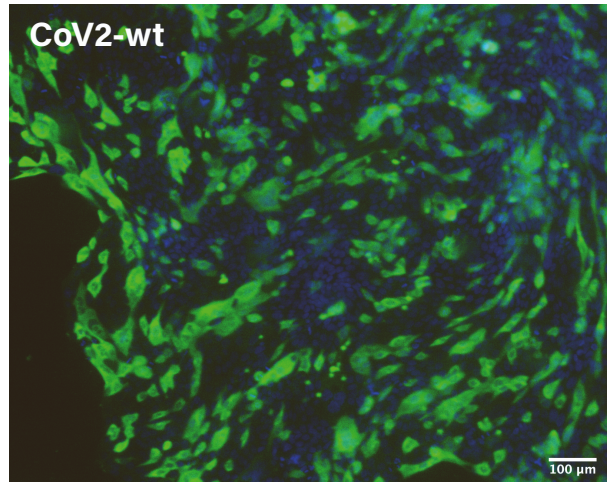
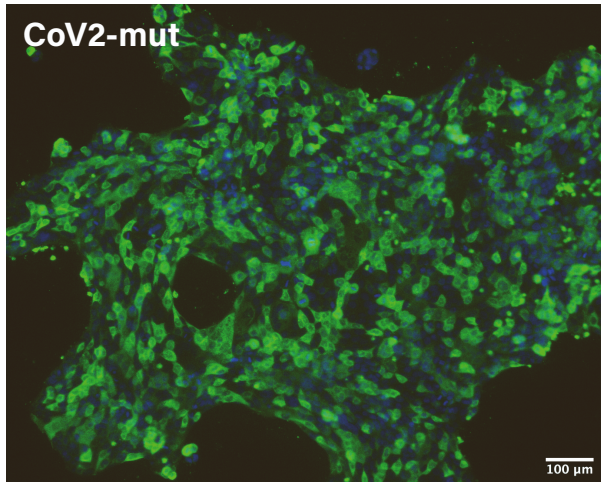
a**b****c**

Figure S4. CoV2-mut characterization, related to Figure 3.

a. RNA reads spanning the deletion region in nsp1 (nt 728-760) in the SARS-CoV-2-WT (CoV2-wt) or in SARS-CoV-2 carrying nsp1- Δ RB mutant (CoV2-mut). **b.** Viral titers in supernatant collected from Calu3 cells infected with CoV2-wt or with CoV2-mut (MOI=0.01) at 1, 2, 3, and 4 dpi. The titers of the CoV2-wt infection were higher than the titers of the CoV2-mut infection at all timepoints (two tailed t-test, where * = $p < 0.01$). Three replicates are presented. **c.** Microscopy images of Calu3 cells infected with CoV2-wt or CoV2-mut at an MOI of 3 at 8hpi stained with antisera against SARS-CoV-2 (green) and DAPI (blue).

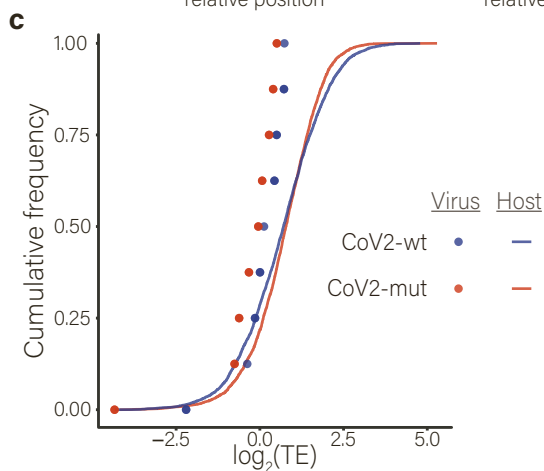
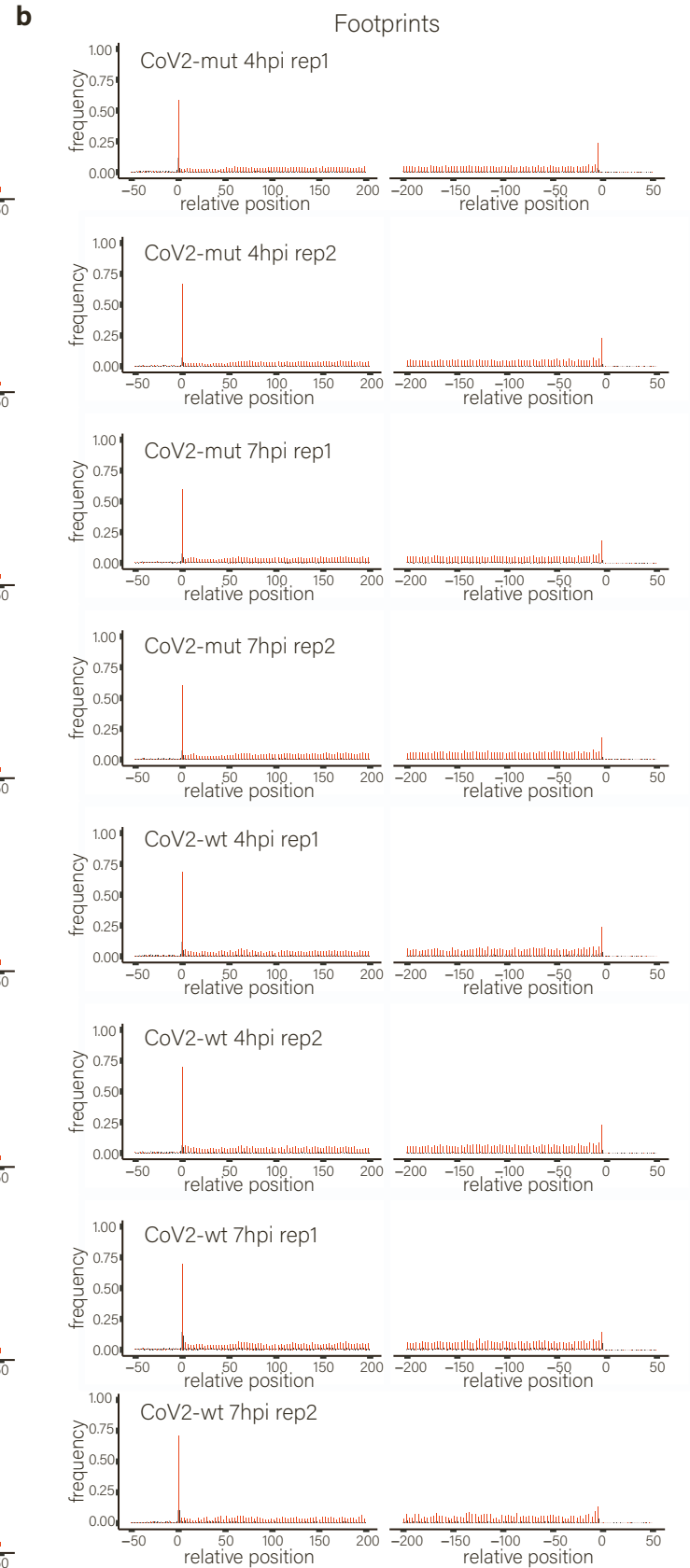
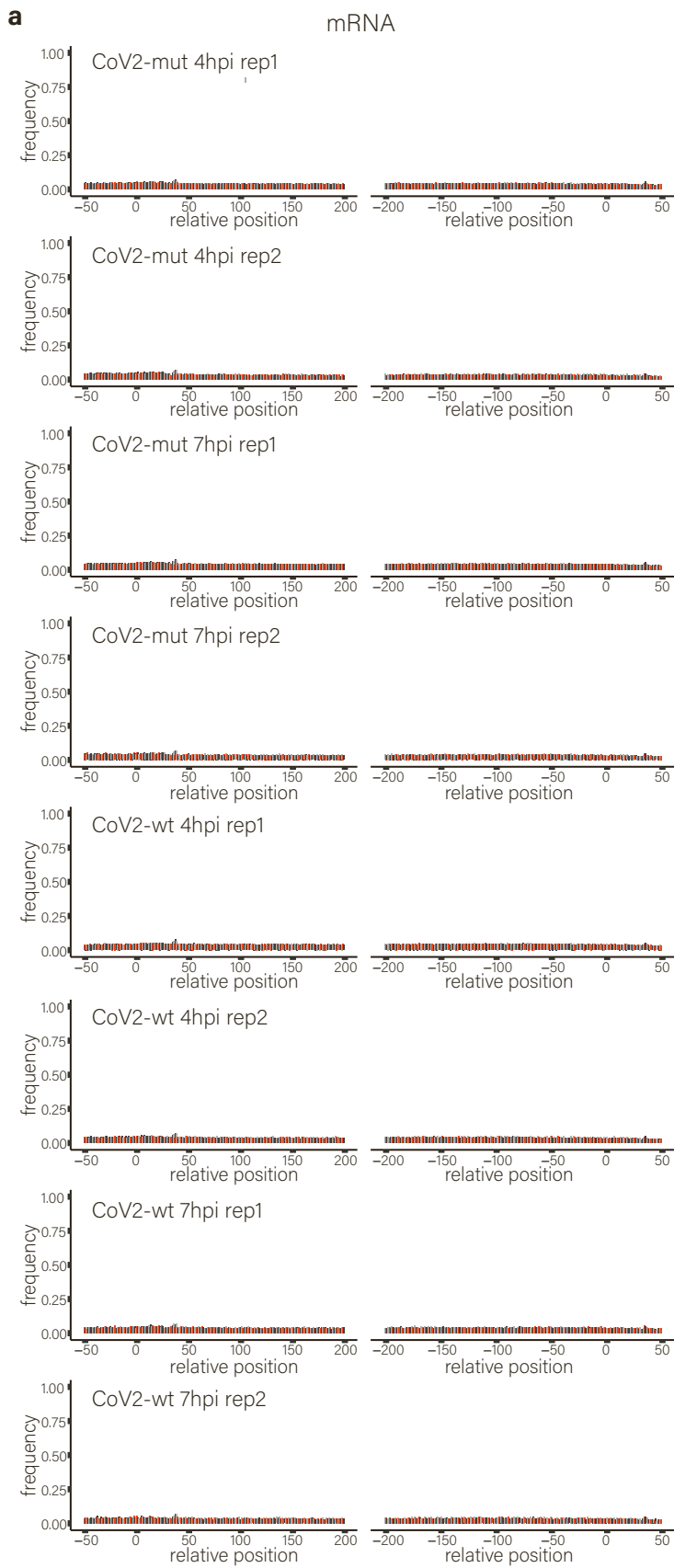


Figure S5. Ribosome profiling measurements in CoV2-wt-infected cells and Cov2-mut-infected cells, related to Figure 4.

a and b. Metagene analysis for the mRNA (**a**) and footprint (**b**) samples. **c.** Cumulative frequency of human (line) and viral (dots) genes according to their relative TE in cells infected with CoV2-wt (blue) or with CoV2-mut (red) at 7 hpi. TE was calculated from ribosome profiling in parallel to mRNA sequencing, and is defined as the ratio of ribosome footprints to mRNA for a given gene. Each dot represents one of nine major viral mRNA species.

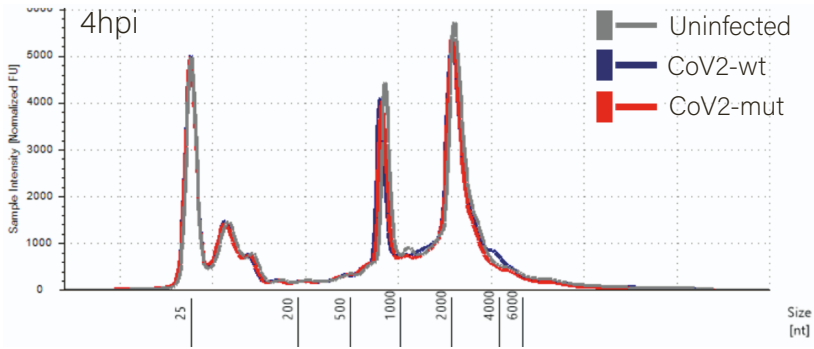
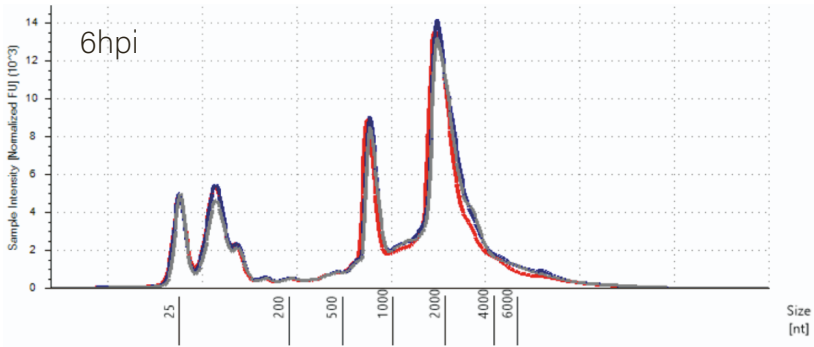
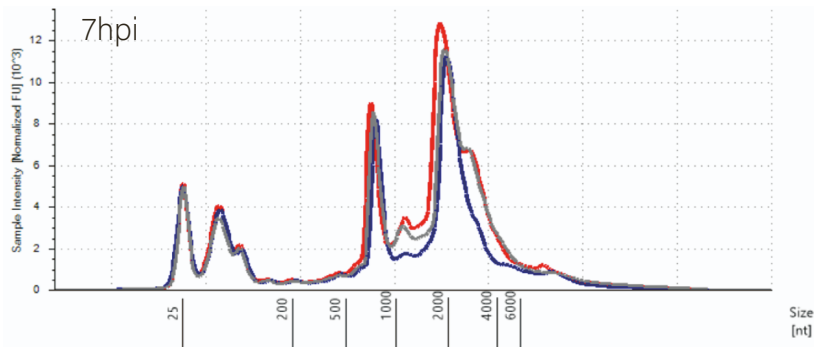
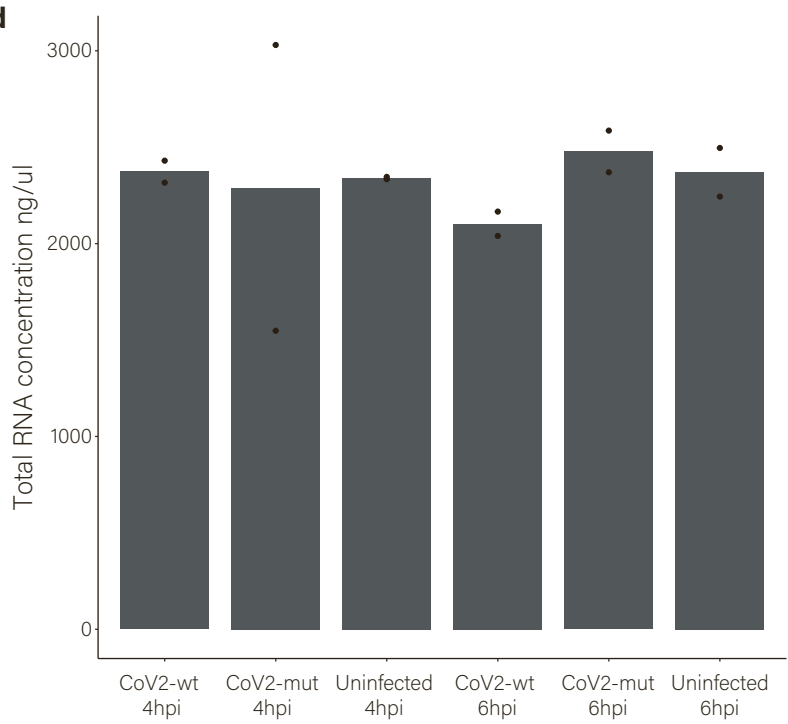
a**b****c****d**

Figure S6. Amounts of RNA in CoV2-wt and CoV2-mut infected cells, related to Figure 5.

a-c. The concentration of the 18S and 28S ribosomal RNAs were measured in uninfected Calu3 cells and Calu3 cells infected with CoV2-wt or CoV2-mut at 4 hpi (a), 6 hpi (b), or 7 hpi (c) by using a TapeStation system. **d.** Total RNA was measured in uninfected Calu3 cells and in CoV2-wt or CoV2-mut infected Calu3 cells at 4 and 6 hpi by Qubit Fluorometer. Two replicates are presented.

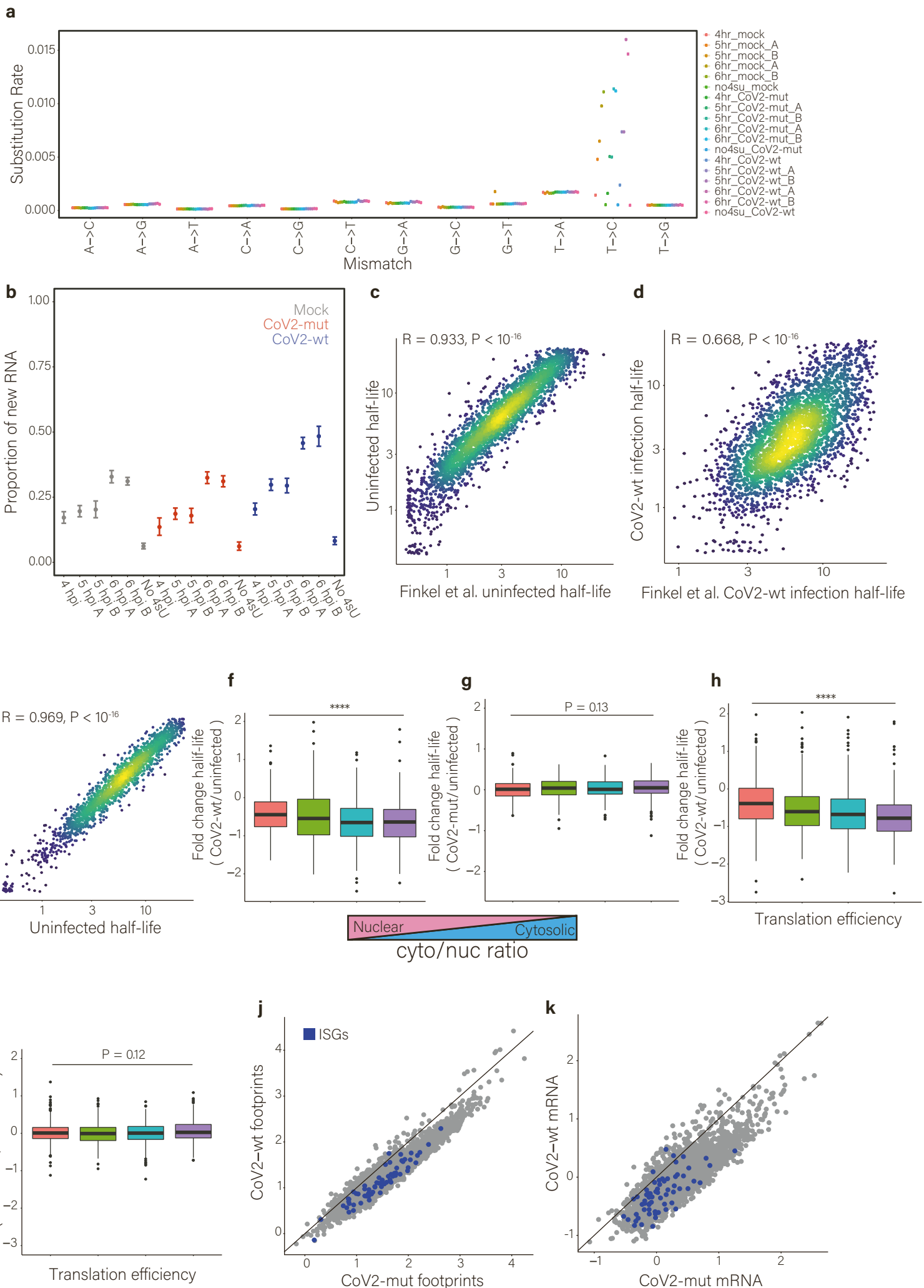


Figure S7. SLAM-seq measurements in CoV2-wt-infected cells and CoV2-mut infected cells, related to Figure 5.

a. Rates of nucleotide substitutions demonstrate efficient conversion rates in 4sU-treated samples compared to non-treated cells (no 4sU). **b.** Proportion of new-to-total RNA (NTR) in Calu3 cells infected with CoV2-wt or CoV2-mut as calculated by GRAND-SLAM(Jürges et al., 2018). **c** and **d.** Scatter plot of transcript half-lives in **(c)** uninfected Calu3 and **(d)** CoV2-wt-infected cells relative to our previous half-lives measurements from uninfected and infected cells (Finkel et al., 2021a). Half-lives lower than 0.8 h or higher than 24h were omitted. Pearson's R and two-sided P value are presented. **e.** Scatter plot of transcript half-lives in CoV2-mut-infected Calu3 cells relative to half-lives in mock infected cells. Pearson's R and two-sided P values are presented. **f-i.** The CoV2-wt/uninfected **(f,h)** or CoV2-mut/uninfected **(g,i)** half-life fold-change compared to the cytosolic/nuclear ratio **(f,g)** or translation efficiency **(h,i)** which are divided into 4 bins. P values for two tailed t-tests between extreme bins are presented, **** = $p < 0.0001$. **j-k.** Scatter plot of footprints **(j)** or mRNA **(k)** measurements in CoV2-wt-infected cells compared to CoV2-mut-infected cells. ISGs are marked in blue.